JOURNAL OF SOLID STATE CHEMISTRY 56, 133–147 (1985)

Neutron Structure Refinement of γ- and β-Lithium Iodate: Comparison between α, γ, and β Phases

J.-M. CRETTEZ AND E. COQUET

Laboratoire d'Optique du Réseau Cristallin, UER MIPC, 6 Bd Gabriel, 21100 Dijon, France

J. PANNETIER AND J. BOUILLOT

Institut Laue-Langevin, 156X, 38042 Grenoble, France

AND M. DURAND-LE FLOCH

Laboratoire de Chimie Minérale D (associé au CNRS No. 254) Faculté des Sciences, Avenue du Général Leclerc 35042, Rennes, France

Received January 3, 1984; in revised form June 29, 1984

Neutron powder diffraction patterns of (γ + α) and β lithium iodate samples are used to refine the structure of γ (at 488 K) and β (at 513 K) $LiIO_3$. All three modifications are built up from Li^+ and $(IO_3)^-$ pyramids but lithium is six-, five-, and fourfold-coordinated to oxygen in the α-, γ-, and β-phases, respectively. The study of IO_3 group displacements through the $\alpha \rightarrow \gamma$ phase transition suggests that the γ phase structure is closely related to a mixed orthohexagonal description of the α structure where both enantiomorphic forms of the hexagonal unit cell are present. The existence of a new α' modification is postulated in view of neutron diffraction and NMR results. A simulation of the structure of hexagonal α-$LiIO_3$ is also presented.

1. Introduction

Three modifications of $LiIO_3$ are known; upon heating, α-$LiIO_3$ transforms reversibly into γ-$LiIO_3$ (at about 500 K with a large hysteresis), then γ-$LiIO_3$ transforms irreversibly into β-$LiIO_3$ (at about 540 K) which is stable up to the melting point (708 K) (*1*). The temperature of the two phase transitions is influenced by the crystal growth conditions (*2, 3*), the nature of the sample (single crystal or powder) and its thermal history (*4*). The structure (hexagonal α-$LiIO_3$ ($P6_3$, $Z = 2$)) has been first determined by Rosenzweig and Morosin (*5*) and De Boer *et al.* (*6*) at room temperature, and the thermal evolution of structural parameters has been recently studied by neutron and X-ray diffraction (*7, 8*). β-$LiIO_3$ can be prepared in two different ways; either by growing single crystals from aqueous solution under specific temperature and pH conditions (*9*), or by heating α-$LiIO_3$ above 540 K which leads to polycrystalline samples. Its structure is tetragonal ($P4_2/n$, $Z = 8$) and was determined by single-crystal X-ray diffraction (*10*).

The present investigation was under-

0022-4596/85 $3.00

taken to determine the crystal structure of γ-$LiIO_3$ and to establish the relationship between the three modifications of lithium iodate. During the completion of this work an orthorhombic structure ($Pna2_1$, $Z = 4$) has been proposed for γ-$LiIO_3$ by Liminga *et al.* (*11*); their results were obtained by profile refinement of X-ray diffraction powder data and the position of lithium atoms cannot be accurately determined. Our results confirm their space group and give a more accurate description of the structure.

The format of this paper is as follows. We first give a description of the experimental procedures used to prepare β- and γ-$LiIO_3$ and to collect neutron diffraction data; in Section 3 we describe the structure of the β-phase and the determination of the structure of γ-$LiIO_3$ from a mixed pattern $\alpha + \gamma$. In Section 4 we shall discuss the structural differences between the three modifications and in Section 5 we shall present a possible model of the $\alpha \rightleftarrows \gamma$ phase transition. NMR results will be presented in Section 6; finally, we shall discuss a simulation of the lattice of hexagonal α-$LiIO_3$ in the last section.

2. Experimental

Neutron powder diffraction patterns were recorded on the D1A high-resolution diffractometer of the Institut Laue-Langevin; the wavelength $\lambda = 1.9066(3)$ Å was calibrated with a Ni powder standard ($a = 3.5238$ Å). The samples were inserted in a cylindrical vanadium container (15 mm in diameter) and the heating device was a conventional furnace with vanadium heater working under low helium pressure. The temperature was measured with a Ni–Cr thermocouple in contact with sample holder. Data were collected from $2\theta = 10$ to 140° in steps of 0.05°. Measurement time was about 15 sec per step. Data of the 10 counters were then summed using a conventional ILL program (*12*).

The powdered sample of β-$LiIO_3$ was obtained by grinding small single crystals; however to avoid a possible contamination of the β powder by small amounts of α-$LiIO_3$ created during grinding in air (*13*), the sample was first heated up to 632 K to ensure a complete transformation into β; then the sample was cooled down to 513 K for measurements.

The powdered sample of γ-$LiIO_3$ was obtained by grinding a large single crystal of α-$LiIO_3$ grown from aqueous solution at pH = 6; this α powder was first heated to 473 K over a period of 3 hr; then the temperature was raised very slowly while measuring the diffraction pattern in the angular range $2\theta = 29$–32° to monitor the intensity of the two reflections $(101)_\alpha$ and $(111)_\gamma$. The temperature was stabilized as soon as the γ line appeared on the pattern (496 K). The sample was held at this temperature for half an hour and then cooled down to 488 K. After a few hours the intensity of $(101)_\alpha$ and $(111)_\gamma$ showed no more evolution with time; the percentage of γ-$LiIO_3$ in the mixture was about 50%. The complete pattern was then recorded over a period of 12 hr. The beginning of the pattern was remeasured at the end of the experiment to ensure that the γ/α ratio did not change during data collection. No line from β-$LiIO_3$ is observed on the final diagram.

The ^7Li NMR spectra were collected on a BRUKER SXP pulse spectrometer operating at 35 MHz in the temperature range RT to 573 K. The powdered samples prepared from a single crystal of α-$LiIO_3$ were contained in Pyrex tubes.

3. Structure Refinements

3.1. β-$LiIO_3$ (513 K)

The Rietveld program (*14*), as modified by Hewat (*15*) was used for profile-fitting structure refinement. Cell parameters are $a = 9.7899(1)$ and $c = 6.1605(1)$ Å. The re-

TABLE I

STRUCTURE DATA OF β-$LiIO_3$ AT 513 K (SPACE GROUP $P4_2/n$, ORIGIN AT $\bar{1}$)

	x	y	z	U_{11}	U_{22}	U_{33}	U_{12}	U_{13}	U_{23}
Li	0.4313(8)	0.2297(7)	0.407(1)	0.064(7)	0.044(4)	0.035(5)	−0.009(4)	−0.025(4)	−0.007(4)
I	0.0349(2)	0.7593(3)	0.1128(4)			Isotropic U = 0.0200(5)			
O(1)	0.8336(3)	0.1205(2)	−0.0574(4)	0.037(2)	0.043(2)	0.080(2)	−0.014(2)	0.012(2)	−0.001(2)
O(2)	0.0823(2)	0.2051(2)	0.1053(3)	0.044(2)	0.059(2)	0.017(1)	0.013(1)	−0.006(1)	0.000(1)
O(3)	0.8430(2)	0.5523(2)	0.1672(3)	0.034(2)	0.052(1)	0.025(1)	−0.022(1)	0.008(1)	0.000(1)

Note. Numbers in parentheses are standard deviations related to the last digit. In three first columns are given fractional position parameters; in last columns anisotropic thermal parameters in Å².

finement started with the atomic parameters given by Schulz (*10*). The neutron scattering lengths were taken from Ref. (*16*). In order to limit the number of parameters to be adjusted, the thermal parameter of iodine is assumed to be isotropic, which is reasonable in view of Schulz's results at room temperature. The other atoms were allowed to vibrate anisotropically. A set of 260 reflections resolved into individual components by the program were used to refine the structural and thermal parameters which are reported in Table I. The final agreement factors for the parameters given in this table are R_N = 0.036, R_P = 0.088, R_{wP} = 0.092, R_{exp} = 0.058. Observed and calculated neutron diffraction profiles are shown in Fig. 1. Results are in satisfactory agreement with Schulz's structure parameters at room temperature except the lithium coordinates which are more accurately determined by neutron diffraction. Bond distances and angles are listed in Table II. By comparison with previous results (*10*), our

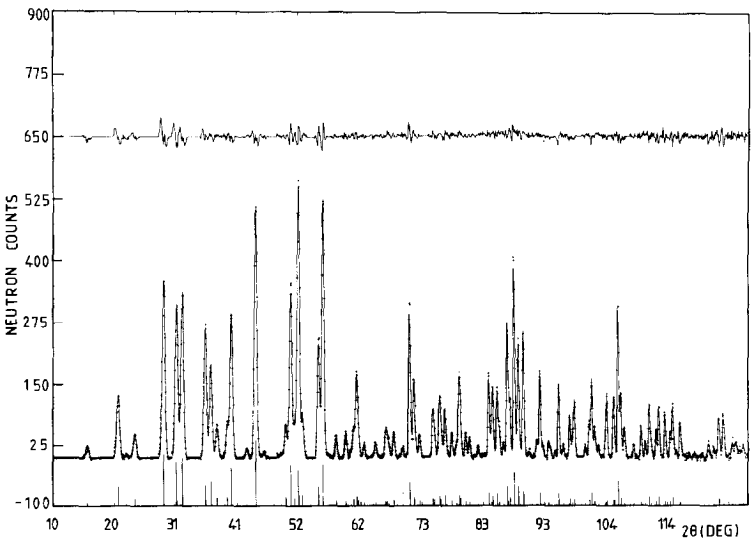

FIG. 1. Diffraction pattern of β-$LiIO_3$ at 513 K. The observed data are indicated by crosses and the calculated profile as solid line.

TABLE II

BOND LENGTHS (Å) AND ANGLES (°) FOR β-$LiIO_3$ AT 513 K

I coordination			
Distances		Angles	
I–O(1^{i})	1.777(3)	O(1^{i})–I–O(3^{i})	100.8
I–O(3^{i})	1.799(3)	O(1^{i})–I–O(2^{i})	101.0
I–O(2^{i})	1.801(3)	O(3^{i})–I–O(2^{i})	99.9
I–O(3^{ii})	2.784(3)		
I–O(1^{ii})	3.005(3)		
I–O(1^{iii})	3.242(3)		
Li coordination			
Distances		Angles	
Li–O(3^{iii})	1.955(7)	O(3^{iii})–Li–O(2^{ii})	120.2
Li–O(2^{ii})	1.968(7)	O(3^{iii})–Li–O(1^{iv})	90.6
Li–O(1^{iv})	1.965(8)	O(3^{iii})–Li–O(2^{iii})	126.5
Li–O(2^{iii})	1.969(8)	O(2^{ii})–Li–O(1^{iv})	114.4
		O(2^{ii})–Li–O(2^{iii})	98.9
		O(1^{iv})–Li–O(2^{iii})	105.7

Note. Atom designations are the same than in Ref. (*10*). Standard deviations are about 0.3° for angles.

data indicate a more regular IO_3 pyramid; in addition, and this is the main difference from Schulz's results, the LiO_4 tetrahedron is almost regular with Li–O distances between 1.955 and 1.969 Å and angles from 90.6 to 126.5°.

3.2. γ-$LiIO_3$ (488 K)

It has not been possible to obtain a pure sample of γ-$LiIO_3$; the diffraction pattern from an 1:1 mixture of α- and γ-lithium iodate was refined with the multiphase profile refinement program of Bendall (*17*). All reflections from $2\theta = 20$ to 144° were used in the refinement; the structure of α-$LiIO_3$ was refined in space group $P6_3$ while for γ-$LiIO_3$ we used the space group $Pna2_1$ determined by Liminga *et al.* (*11*). This acentric space group is actually supported by the result of second harmonic generation (SHG) measurements above the $\alpha \rightarrow \gamma$ transition temperature: at the transition the strong SHG signal from α-$LiIO_3$ decreases to about a third of its value (*18*); then it decreases slowly with increasing temperature to disappear abruptly at the $\gamma \rightarrow \beta$ phase transition. The starting parameters (cell dimensions and atomic coordinates) were taken from Refs. (*8, 11*) for α- and γ-$LiIO_3$, respectively; all atoms were compelled to vibrate isotropically except the oxygen of the α-phase; the three halfwidth parameters U, V, and W were constrained to the same values for both phases. Gaussian peaks were assumed for both phases. Refinement of instrument (zero shift, U, V, and W) and structural (cell dimensions, atomic coordinates, and Debye–Waller factors) parameters together with the two scale factors led to

$$R_N = 0.095,\ R_P = 0.168,\ R_{wP} = 0.174,$$

to be compared with $R_{expected} = 0.048$. The isotropic thermal parameters of lithium and iodine in α-$LiIO_3$ refined to negative values. Detailed examination of the difference profile then revealed that most of the discrepancies could be attributed to the α-$LiIO_3$ pattern. The poor fit of the calculated profile to the experimental α-$LiIO_3$ lines is observed either on the intensities or on the full-widths at half-maximum (FWHM) or on both parameters. A second refinement was then performed with two sets of halfwidth parameters $(U,V,W)_\alpha$ and $(U,V,W)_\gamma$ but did not decrease significantly the agreement factors ($R = 0.094$, $R_p = 0.162$, $R_{wP} = 0.167$). However, whereas the profile parameters of the γ-phase retained reasonable values corresponding to the resolution function of the diffractometer ($U_\gamma = 2615$, $V_\gamma = -6616$, $W_\gamma = 5149$), the profile parameters of α-$LiIO_3$ refined to rather different values ($U_\alpha = 1375$, $V_\alpha = -3961$, $W_\alpha = 3718$). In addition, examination of a few single (or almost single) reflections of the α-phase showed that all the experimental

TABLE III

STRUCTURE DATA OF γ-$LiIO_3$ AT 488 K (SPACE GROUP $Pna2_1$)

	x	y	z	B
Li	−0.0236(10)	−0.0901(15)	0.0086(41)	4.9(3)
I	0.3203(3)	0.0733(5)	0.	0.8(1)
O(1)	0.1499(3)	0.0231(6)	−0.1842(9)	2.9(1)
O(2)	0.4269(4)	−0.1447(5)	−0.1685(13)	3.8(1)
O(3)	0.3738(4)	0.3147(6)	−0.1891(12)	2.9(1)

Note. Isotropic thermal parameters (in Å^2) are given in the last column.

FWHM's are not yet correctly reproduced by these new parameters which suggests that the simple Cagliotti's equation (*19*)

$$(\text{FWHM})^2 = U\tan^2\theta + V\tan\theta + W$$

may not apply to the pattern of α-$LiIO_3$ in the mixed sample α + γ. This could result from a high concentration of planar defects in α-$LiIO_3$ at this temperature (see below) or from anisotropic strains on the crystallites arising from the large volume change occurring at the transition; indeed the consequence of such effects is that the FWHM's are no longer a simple instrumental parameter but depends also on the scattering vector; this means that the standard Rietveld method of profile analysis can no longer be used. Unfortunately it has not been possible to isolate enough single and well-defined reflections of α-$LiIO_3$ from the pattern to analyze further their shape as a function of (*hkl*). Moreover, the mixing of the two patterns of α- and γ-$LiIO_3$ is such that it is not possible to exclude all the α-phase lines to refine only the structure of γ-$LiIO_3$. We then adopted the following procedure:

—We first tried to obtain a best fit to the experimental pattern by introducing a few other parameters in the refinement of the α-phase (asymmetry parameters, I and Li occupancy factors). Although one cannot expect these refined parameters to achieve any physical significance, they have been used to obtain the "best numerical fit" to the profile of the α-phase within the constraint of the Rietveld's method (Gaussian peak shapes, no dependence of FWHM on the scattering vector).

—The "observed" intensities of γ-$LiIO_3$ obtained as a result of the profile refinement have subsequently been used for a conventional structure refinement; however all the lines which were close to poorly fitted lines of the α-phase were excluded from this last refinement. Cell parameters are a = 9.4039(4), b = 5.8539(3), and c = 5.2915(3) Å. The final refined parameters are given in Table III. They do not differ significantly from the results of the last Rietveld refinement, but we consider that the above procedure leads to a more correct estimate of the standard deviations and agreement factors (R = 0.060, R_w = 0.045). Calculated distances and angles are given in Table IV.

TABLE IV

BOND LENGTHS (Å) AND ANGLES (°) FOR γ-$LiIO_3$ AT 488 K

Distances		Angles	
I coordination			
I–O(3)	1.803(5)	O(1)–I–O(2)	96.0
I–O(2)	1.852(5)	O(1)–I–O(3)	94.1
I–O(1)	1.899(5)	O(2)–I–O(3)	97.0
I–O(3^{ii})	2.887(5)		
I–O(2^{ii})	2.984(5)		
I–O(1^{ii})	3.131(5)	O(1^{i})–Li–O(2^{i})	102.6
		O(1^{i})–Li–O(3^{i})	86.2
Li coordination		O(1^{i})–Li–O(3)	82.6
		O(1^{i})–Li–O(1^{ii})	143.1
Li–O(2^{i})	1.872(14)	O(2^{i})–Li–O(3^{i})	108.2
Li–O(1^{i})	2.036(14)	O(2^{i})–Li–O(3)	105.5
Li–O(1^{ii})	2.051(19)	O(2^{i})–Li–O(1^{ii})	114.3
Li–O(3)	2.151(14)	O(3^{i})–Li–O(3)	146.1
Li–O(3^{i})	2.204(18)	O(3^{i})–Li–O(1^{ii})	81.0
Li–O(2^{ii})	3.247(14)	O(3)–Li–O(1^{ii})	89.0

Atom designations

		Li	$\frac{1}{2}+x, \frac{1}{2}-y, z$
O(1^{i})	$\frac{1}{2}+x, \frac{1}{2}-y, z$	O(1^{ii})	$\frac{1}{2}-x, \frac{1}{2}+y, \frac{1}{2}+z$
O(2^{i})	$x, 1+y, z$	O(2^{ii})	$1-x, \bar{y}, \frac{1}{2}+z$
O(3^{i})	$1-x, 1-y, \frac{1}{2}+z$	O(3^{ii})	$\frac{1}{2}-x, y-\frac{1}{2}, \frac{1}{2}+z$

Note. For atom designations refer to Table III. The eds's of O–I–O angles are about 2°.

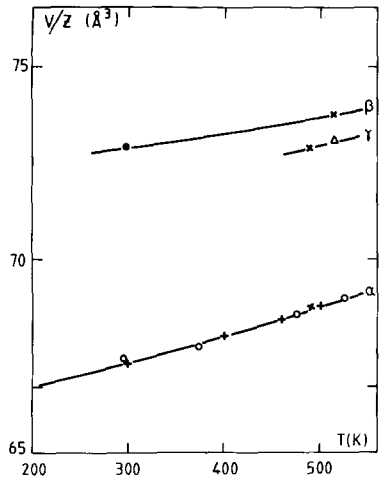

FIG. 2. Volume per formula unit for α-, γ-, and β-$LiIO_3$ as a function of temperature. (×) This work, (+) Ref. (*7*), (○) Ref. (*8*), (●) Ref. (*10*), (△) Ref. (*11*).

4. Comparison between α-, β-, and γ-$LiIO_3$ Modifications

A first difference between the 3 phases of lithium iodate lies in the volume per formula unit; as shown in Fig. 2, the largest volume change occurs at the $\alpha \rightarrow \gamma$ transition ($\Delta V = 4.2$ Å^3) which explains the destruction of the α-$LiIO_3$ single crystal during the phase transition. All three modifications of lithium iodate are built up from discrete (IO_3) groups and lithium atoms; in addition each iodine atom is linked to three other oxygen at distances in the range 2.8 to 3.2 Å. In order to compare the deformation of the lithium and iodine coordination polyhedra for the three modifications we make use of the distortion index (DI) introduced by Brown and Shannon (*20*):

$$\mathrm{DI} = \frac{10^6}{n} \sum_{i=1}^{n} \left(\frac{d_i - \langle d \rangle}{\langle d \rangle} \right)^2$$

where n is the coordination number, d_i the length of the ith bond, and $\langle d \rangle$ the average bond length. Average geometrical parameters and distortion indices for α-, γ-, and β-$LiIO_3$ are listed in Table V.

Iodate groups form regular trigonal pyramids in the α phase but distorted ones in β- and γ-modifications. Average bond lengths and angles within the (IO_3) pyramid are almost identical in α- and β-$LiIO_3$ and in good agreement with the values observed in other iodate structures. The average I–O distance in γ-$LiIO_3$ is larger than the usual values and cannot be explained simply on the basis of the well known increase of the average bond length with distortion (*20*).

The main difference between the three modifications of lithium iodate lies in the lithium environment. Indeed in the α phase the lithium atoms are sixfold-coordinated to oxygen to form an octahedron with two sets of almost equal Li–O distances: 2.094 and 2.167 Å at 475 K (*8*). In the γ-modification, the lithium is clearly fivefold-coordinated with distances ranging from 1.87 to 2.20 Å; the next Li–O distance (the sixth bond in the α-phase) is at 3.25 Å. The average bond

TABLE V

AVERAGE BOND LENGTHS (Å) AND ANGLES (°) FOR IODINE AND LITHIUM OXYGEN ENVIRONMENTS IN THE THREE PHASES OF $LiIO_3$; DISTORTION INDICES OF IODATE AND LiO_n POLYHEDRA

Phase	T (K)	⟨I–O⟩	⟨I---O⟩	⟨O–I–O⟩	DI (IO_3)	CN(Li) (n)	⟨Li–O⟩	DI (LiO_n)
α	475	1.801	2.947	100.5	0	6	2.130	294
γ	488	1.851	3.001	95.7	448	5	2.06	3054
β	513	1.792	3.010	100.6	37	4	1.964	8

length is 2.06 Å as compared with the value of 2.07 Å found in lithium metaborate $LiBO_2$ where lithium is also in fivefold-coordination (*21*). In β-$LiIO_3$, lithium is tetrahedrally coordinated with four nearly equal bonds from 1.955 to 1.969 Å; the average bond distance is 1.964 Å close to the value 1.960 Å found in Li_2CO_3 for instance (*22*).

Another way to analyze the three phases of lithium iodate is to calculate the distribution of bond valences of the two cations between their surrounding oxygen atoms. This concept of bond valence, originally introduced by Pauling (*23*), has recently been refined by a number of workers (for a recent review of the subject, see, for instance, Ref. (*24*)). The most commonly used analytical relations between bond strength s_i and bond length d_i are the inverse power law (*20*) and the logarithmic function (*25, 26*). We used the latter expression

$$s_i = \exp \frac{d_0 - d_i}{B},$$

where d_0 (the length of a bond of unit valence) and B are fitted constants. From a survey of the literature we selected 25 Li^+ and 46 I^{5+} environments (oxides only) with accurately determined bond distances (esd(d_i) $\leq$ 0.01 Å). The valence parameters d_0 and B corresponding to the Li^+–O and I^{5+}–O were then obtained by a statistical procedure similar to that described by Brown and Shannon (*20*) giving

$$Li^+\text{–O: } d_0 = 1.282 \text{ Å}, B = 0.480 \text{ Å}$$
$$I^{5+}\text{–O: } d_0 = 1.982 \text{ Å}, B = 0.401 \text{ Å}.$$

These parameters have been used to calculate the bond strength sums given in Table VI. The valence sum rule is well obeyed by all three lithium environments. This is also true for the iodine environment in α- and β-$LiIO_3$ but rather large discrepancies are observed for I,O(1) and O(2) in γ-$LiIO_3$; this is obviously a consequence of the rather large I–O(1) and I–O(2) distances (Table IV) calculated for this structure.

TABLE VI

ANALYSIS OF BOND VALENCES IN THE THREE PHASES OF LITHIUM IODATE

α	Li	I	Σs
O	0.189 0.163	1.564 0.100	2.016(6)
Σs	1.055(7)	4.99(2)	
β	Li	I	Σs
O(1)	0.241	1.668 0.078 0.043	2.03(2)
O(2)	0.239 0.239	1.572	2.05(2)
O(3)	0.246	1.579 0.136	1.96(2)
Σs	0.96(2)	5.08(4)	
γ	Li	I	Σs
O(1)	0.208 0.201	1.231 0.057	1.70(3)
O(2)	0.292	1.384 0.083	1.76(3)
O(3)	0.163 0.146	1.564 0.105	1.98(3)
Σs	1.01(3)	4.42(6)	

Note. Expected valences: Σs = 5(iodine), 2(oxygen), 1(lithium) valence units. Values in parenthesis are valence esd's as estimated from bond length esd's.

5. A Geometrical Description of the $\alpha \rightleftarrows \gamma$ Transformation

X-Ray diffraction studies of the $\alpha \rightarrow \gamma$ transition (*4*) have shown that the two cells are related as

$$a_\gamma \simeq a_\alpha\sqrt{3};\ b_\gamma \simeq a_\alpha;\ c_\gamma \simeq c_\alpha$$

then a possible relation between the two structures may conveniently be examined in terms of this orthohexagonal cell. Projection of the structures of α- and γ-phases along the **c** axis are shown in Figs. 3a and c, respectively. As discussed in the previous section the trigonal pyramidal iodate ions are only slightly affected by the transition;

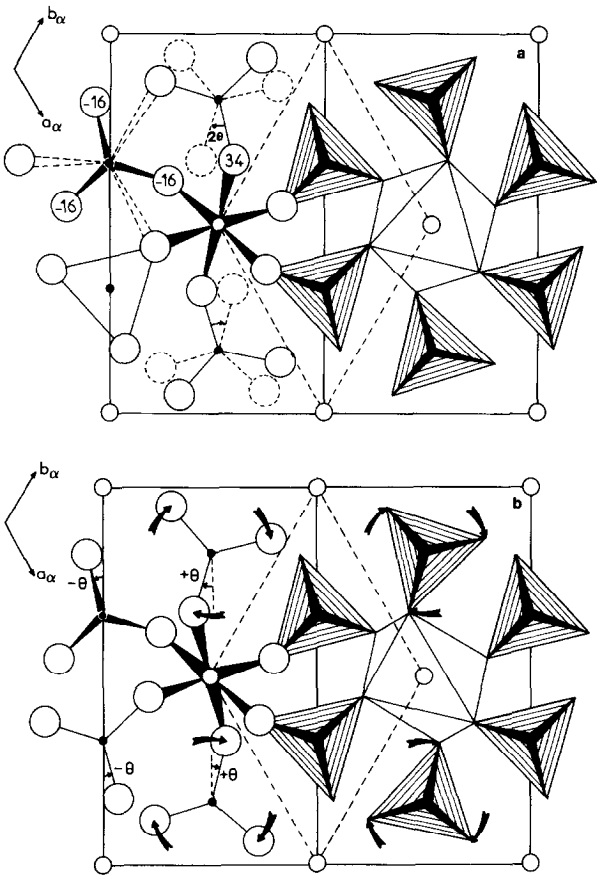

FIG. 3. (a) Projection along the c-axis of the orthohexagonal cell of α-$LiIO_3$ (two unit cells). Dashed outline represents the hexagonal cell. Pyramidal iodate ions are shaded; small open circles denote the lithium atoms; solid and dashed line threefold stars on the left-hand unit cell represent the orientations of (IO_3) groups in the two enantiomorphic configurations. (b) Hypothetical "mixed α-$LiIO_3$" structure (same orientation and notation as (a): The (**a,c**) layers containing Li and IO_3 groups correspond alternatively to the L- and D-forms of α-$LiIO_3$. Arrows indicate the rotation of the IO_3 groups from α-$LiIO_3$. (c) Projection along the c-axis of the structure of γ-$LiIO_3$ (notation as above). Arrows indicate the shifts of Li^+ and $(IO_3)^-$ from (b). (d) Proposed structure of a domain wall in α-$LiIO_3$.

then, except for small changes in the unit-cell dimensions, the main differences between the α- and γ-phase structures must arise from a modification of packing of these iodate pyramids and from the resulting change of lithium coordination. Examination of Figs. 3a and c shows that the transformation $\alpha \rightarrow \gamma$ results from (i) a rotation by $2\theta \sim 30°$ around **c** of half of the pyramids, (ii) a cooperative shift of iodate groups alternatively along $+\mathbf{b}_\gamma$ and $-\mathbf{b}_\gamma$.

This reorientation of the IO_3 pyramids may be related to the distortion of α-$LiIO_3$. Indeed α-$LiIO_3$ structure shows a small deviation from a regular hexagonal packing (for instance see Fig. 4 of Ref. (*27*)). A measure of this distortion is provided by the angle θ (see Fig. 3a and discussion below); this angle which is slightly temperature dependent (*8*) can be positive or negative and this leads to two configurations of opposite chirality. Then, according to the above

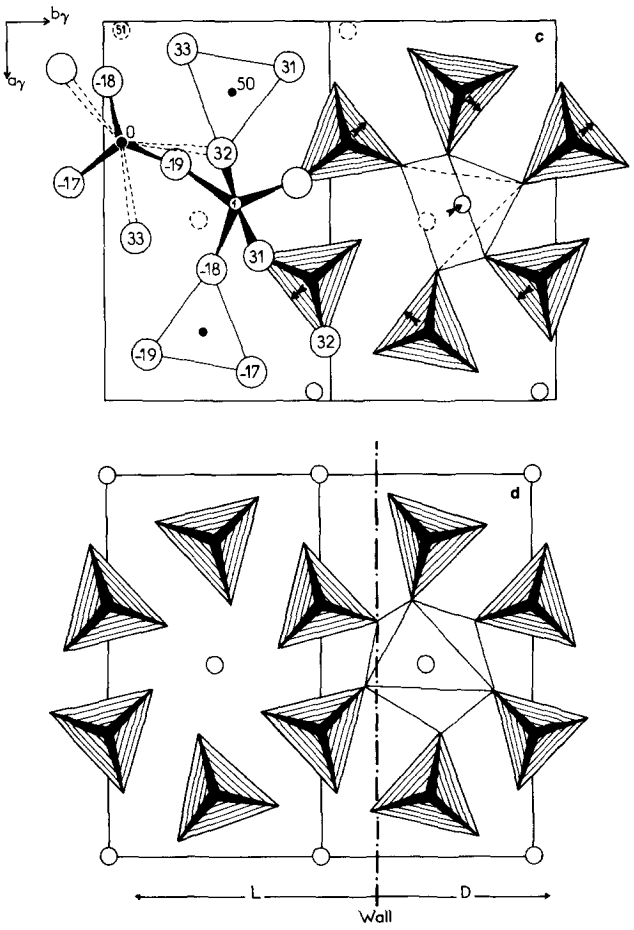

FIG. 3—*Continued.*

mentioned rotation of half of the (IO_3) groups, γ-$LiIO_3$ can be described as built up from a succession of α-$LiIO_3$ cells belonging alternatively to the D- and L-enantiomorphs. This is best seen by comparing Figs. 3c and b which represents an hypothetical "mixed" α-$LiIO_3$ structure in which the iodate pyramids are alternatively rotated about the threefold axis by $+\theta$ and $-\theta$ from the position corresponding to the regular hexagonal packing. However, such a structure gives rise to (i) short oxygen–oxygen distances between two iodate groups and (ii) a geometrical arrangement of the iodine atoms which is not favorable from the point of view of secondary bonding.

Starting from this "ideal" mixed structure, small cooperative shifts of the (IO_3) pyramids (shear plane perpendicular to $\mathbf{a}_\gamma$) and small tilts (~3°) from the **c** axis give the structure of γ-$LiIO_3$. The main result of this relaxation from the "mixed" structure to the arrangement of pyramids found in γ-$LiIO_3$ is a change of the lithium environment from a distorted octahedron (Fig. 3b) to a fivefold polyhedron (Fig. 3c). A second consequence of this rearrangement is a drastic change of cell parameters with a contraction of the orthohexagonal axis *a*

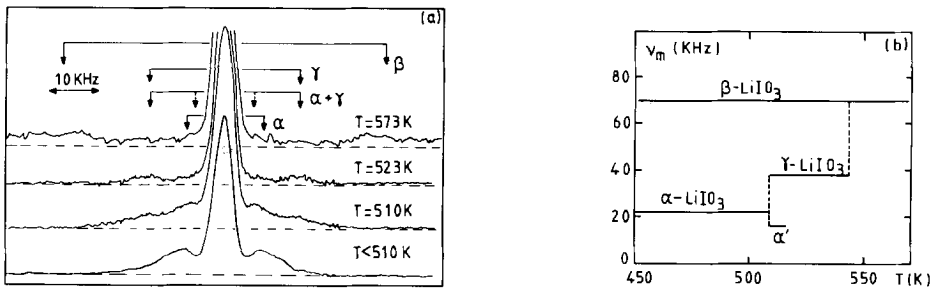

FIG. 4. (a) ^{7}Li NMR patterns of the three phases of $LiIO_3$. (b) Evolution of the NMR signal versus temperature.

from 9.5472 Å in α to 9.4093 Å in γ and an expansion of the orthohexagonal axis b from 5.5121 Å in α to 5.8539 Å in γ. This is to be related to the analysis of the IR spectra (*28, 29*): the normal modes assigned to IO_3 group displacements in this model of the $\alpha \rightarrow \gamma$ phase transition exhibit a strong increase of damping coefficients in the vicinity of the phase transition. Indeed:

(i) The external ν_1^A mode (148 cm^{-1} at room temperature (RT)) corresponds to rotations of IO_3 groups around the **c** axis.

(ii) The external ν_1^{E1} mode (176 cm^{-1} at RT) to rotations of IO_3 groups around an axis perpendicular to the **c** axis (related to the tilts of pyramids from the **c** axis).

(iii) The external part of the mixed internal–external ν_3^{E1} mode (355 cm^{-1} at RT) can be associated to the relative translations of IO_3 groups with respect to lithium atoms in the (**a**,**b**) plane.

This description of the $\alpha \rightarrow \gamma$ phase transition is also further supported by a recent investigation of the structure of defects in neutron-irradiated α-$LiIO_3$ crystals (*30*); indeed this optical study has shown the occurrence of linear periodic nonuniformities (concentration of defects) in such crystals. These nonuniformities are 300 to 400 μm apart and make an angle of 30–40° with the hexagonal axis, i.e., they almost coincide with the **a** axis of the orthohexagonal cell. This strongly suggests that these defects correspond to walls between enantiomorphic domains of α-$LiIO_3$ (Fig. 3d); although the barrier of potential which corresponds to $\theta = 0°$ is probably rather high (see below), the structure of γ-$LiIO_3$ shows that the lattice can easily accommodate different orientations of the (IO_3) pyramids and that a likely frontier between two domains (D- and L-domains) is a plane perpendicular to the **b** axis of the orthohexagonal cell. Therefore the high density of defect specimen studied by Klimova *et al.* (*30*) is a partly ordered crystal intermediate between ideally perfect α-$LiIO_3$ and γ-$LiIO_3$; or, to say it another way, γ-$LiIO_3$ might be considered as a fully ordered highly defective α-$LiIO_3$.

6. NMR Investigations

^{7}Li NMR results clearly show up the differences between the three phases of $LiIO_3$ (Fig. 4a). The ^{7}Li satellites are observed in all three phases and the quadrupole splitting increases in the order $\alpha < \gamma < \beta$ indicating an increased distortion[1] of Li^+ environment in the same order. This result can be correlated more quantitatively with the structural results by calculating the electric field gradient (EFG) tensor at the lithium site for all three structures. Indeed, for ^{7}Li

[1] Here the term distortion concerns the electric field gradient at the lithium site, i.e., a rather long-range interaction; it must not be confused with the distortion quoted in Table V which refers to the first sphere of coordination only.

(spin $I = \frac{5}{2}$) the strength of the quadrupole interaction (*31*) can be measured as

$$\nu_Q = 3eV_{ZZ}Q/2I(I-1)h, \qquad (1)$$

where Q is the ^{7}Li nuclear quadrupole moment, and V_{ZZ} the principal component of the EFG tensor. However, the powder spectrum of such a quadrupolar nucleus only allows to measure the product $\nu_m = \nu_Q(1-\eta)$ where η is the asymmetry parameter defined as

$$\eta = (V_{XX} - V_{YY})/V_{ZZ}.$$

The usual definition $|V_{ZZ}| \geq |V_{YY}| \geq |V_{XX}|$ limits the η values to the range [0,1].

In ionic crystals the main contribution to the field gradient comes from the lattice, i.e., from the arrangement of the ionic charges around a given site and the nine (five independent) components of the EFG tensor can be calculated from the relation

$$V_{ij} = \sum_k q_k \sum_i \sum_j (3r_{ik}r_{jk} - \delta_{ij}r_k^2)/r_k^5, \qquad (2)$$

where

$$i,j = x, y, z$$
$$\delta_{ij} = 1 \quad \text{if } i = j \text{ and 0 otherwise}$$

and r_{xk}, r_{yk}, r_{zk} are the coordinates in an arbitrary orthogonal system of the kth atom with charge q_k situated at the distance r_k from the reference site.

The conditionally convergent series of Eq. (2) can be evaluated either by direct summation or, after transformation, by summation in Fourier space (*32*). In the former method the convergence of the lattice sums can be improved by making use of the unit-cell-shaped boundary method (*33*) and extrapolating to infinity by a so-called Neville-plot (*34*). Both methods converged to the same values and direct summation was used for most of the calculations mentioned below.

In the following, lithium iodate is considered as an ionic crystal $Li^+(IO_3)^-$ which means first that we do not take into account the contribution of lone-pairs to the EFG. The hypothesis of a onefold positively charged lithium is reasonable and supported by recent investigation of somewhat similar crystals (e.g., see $LiBO_2$ (*21*)); then evaluation of the field gradients in the three phases of $LiIO_3$ depends on knowledge of the charge distribution inside the iodate group: $I^{+q}O_3^{-(1+q)/3}$. The electrostatic field gradient at a lithium site in α- and β-$LiIO_3$ was calculated as a function of the effective charge q of iodine; the calculated tensors were diagonalized in order to obtain V_{ZZ} and η (note that the axial symmetry at the Li^+ site in α-$LiIO_3$ implies that $\eta^\alpha = 0$). The charge distribution in the $(IO_3)^-$ was then simply obtained by comparing the experimental ratio $\nu_m^\alpha/\nu_m^\beta = 22$ kHz/70 kHz = 0.314 to the calculated $V_{ZZ}^\alpha/V_{ZZ}^\beta(1-\eta^\beta) = f(q)$. Agreement with the experimental ratio[2] is found for $q = +2.3$ which is to be compared with the value $q = 2.25$ (±0.10) obtained from X-ray chemical shifts (*35*). The corresponding asymmetry parameter is $\eta^\beta = 0.376$. The numerical relation between ν_m (expected) and the calculated EFG tensor for $q = 2.3$ can then be written

$$\nu_m = 800(1-\eta)V_{ZZ},$$

with ν_m and V_{ZZ} in units of kiloHertz and $e \cdot (\text{Ångstrom})^{-3}$, respectively. Using this relation and the above charge distribution in $(IO_3)^-$ one obtains for γ-$LiIO_3$ a calculated value of 59 kHz; owing to the crudeness of the charge model and to the uncertainties in the experimental values of ν_m^β and ν_m^α, this is

[2] A similar calculation has recently been published by Daraselia and Bräuer (*46*), giving a rather different charge distribution on the iodate group; however their method of calculation makes use of the Sternheimer antishielding factor $(1-\gamma_\infty)$ and of the ^{7}Li quadrupole moment Q for which no accurate value is available. In order to overcome this difficulty we based our calculation on ν_m^α/ν_m^β which does not depend on these two parameters; hence errors in our estimated charge distribution arises only from the uncertainties of ν_m^α/ν_m^β and from the model of charge distribution.

in reasonable agreement with the measured value $\nu_m^\gamma = 38$ kHz.

A second interesting feature of the ^{7}Li NMR in $LiIO_3$ is the evolution of the signal between 509 and 543 K, i.e., in the range of temperature where γ-$LiIO_3$ is observed (Fig. 4b):

(i) Up to 509 K one observes only two satellite lines with a splitting $\nu_m = 22$ kHz typical of α-$LiIO_3$ (*36*). This splitting is almost temperature independent. In this range of temperature the spin-lattice relaxation time T_1 decreases (from 83 sec at 473 K to 32 sec at 509 K) as already observed by other authors (*37*).

(ii) Between ~509 and 514 K two pairs of satellites are observed (Fig. 4a): the first shows a splitting of about 38 kHz and is observed up to 543 K (i.e., up to the transition to β-$LiIO_3$); therefore it is attributed to γ-$LiIO_3$. The second set of satellites gives a much smaller splitting (~16 kHz) and its intensity decreases rapidly when the temperature is raised: it is no longer observed above 514 K. As long as β-$LiIO_3$ is not formed, all these transformations are completely reversible. In this narrow range of temperature two spin-lattice relaxation times T_1 are observed ($T_1 \simeq 49$ sec and $T_1' \sim 3$ sec at 509 K).

(iii) Above 543 K the sample is irreversibly transformed into β-$LiIO_3$. The β-$LiIO_3$ quadrupole splitting (70 kHz) is also temperature independent.

These results suggest that the transition from α- to γ-$LiIO_3$ proceeds through an intermediate phase which we call α'-$LiIO_3$. The exact nature of this phase, the domain of stability of which is very narrow, is not known and it has not been directly observed in diffraction experiments. However, we already mentioned in Section 3.2 that all our attempts to refine the structure of a α-$LiIO_3$ in space group $P6_3$ failed. This may indicate that the structure of α is modified when γ-$LiIO_3$ is being formed. NMR results bring evidence that Li^+ is much more mobile in this phase than in α-, γ-, or β-$LiIO_3$. As the $\alpha \rightarrow \gamma$ transition is a reconstructive transformation which involves a modification of the first sphere of coordination of Li atoms, this α'-$LiIO_3$ might well be an amorphous or, at least, very divided phase as already observed in similar phase transitions (*38*). Further information on this point could only be obtained through a detailed quantitative investigation of the phase transformation in the range 509–515 K.

7. Discussion

The above description of the relationship between the α- and γ-$LiIO_3$ structures has emphasized the importance of the prototype structure of α-$LiIO_3$ which would correspond to a regular hexagonal close packing ($\theta = 0°$). Although this ideal structure is never realized by lithium iodate, studies of the structural temperature dependence in α-$LiIO_3$ have shown (*7, 8*) that θ decreases regularly from 15.69° at 20 K to 14.55° at 500 K; moreover the analysis of thermal motion shows that iodine atoms vibrate almost isotropically whereas the thermal vibrations of oxygen are rather anisotropic with a principal component close to the (**a,b**) plane. All these arguments suggest that the rotation about the trigonal axis of the IO_3 pyramids is a soft feature of the hexagonal structure and that the variation of the potential energy of an iodate group as a function of the angle of rotation θ can be represented by a double well potential (Fig. 5a).

The two minima of energy are about 30° apart and E_i is the energy barrier for cooperative rotation of all iodate groups of the lattice from one enantiomorphic form to the other. An exact calculation of this potential curve, even with a simple lattice model, would require a knowledge of many parameters (e.g., the repulsive interaction parameters in the case of an ionic Born–Mayer model). However, it is possible to

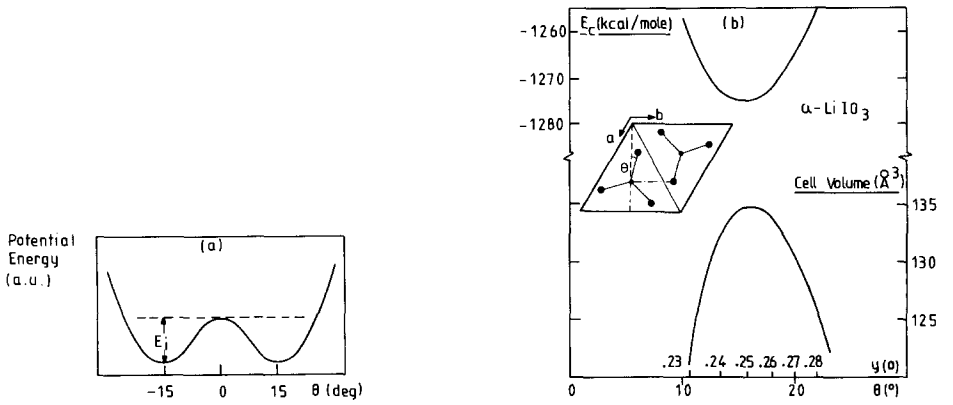

FIG. 5. (a) Double well potential versus angle of rotation θ. (b) DLS simulation of the distortion of α-$LiIO_3$. The angle θ which measures the deviation from a regular hexagonal close packing is defined in the insert. Parameters of simulation are given in Table VII.

further investigate this aspect in a rather simple way by making use of a computer simulation procedure. Indeed a common feature to all the known iodate structures is the occurrence of two sets of iodine–oxygen distances: each iodine atom is linked to three oxygen atoms at a distance of about 1.80 Å with average O–I–O angle of 99°; in addition to these strong (short) bonds there are invariably two, three, or four weak bonds at distances in the range 2.7–3.0 Å. This irregular environment is a result of the steric activity of I^{5+} lone-pair and the coordination of I atom in iodates is often considered (*39*) as octahedral with the iodine atom displaced off-center along the threefold axis. This information was input in a distance least-squares program DLS-76 (*40*)[3] in order to simulate the structural evolution of hexagonal lithium iodate as a function of the rotation angle θ; the input parameters are given in Table VII. With these constraints, one can simulate the α-$LiIO_3$ lattice in the range $10 < \theta < 23°$ but it is not possible to obtain a solution for $\theta < 10°$ and in particular for $\theta = 0$. The variation of the calculated cell volume as a function of θ is given in Fig. 5b. A first important result from that simulation is that the experimentally observed structure ($\theta \sim 15°$) corresponds to the maximum cell volume. This is a good example of a general rule recently introduced by O'Keeffe (*44*) which states that "ionic structures are expected to be those of maximum volume subject to the constraint of fixed bond lengths." This is further supported by a calculation of electrostatic (Madelung) energy E_c[4]: as ex-

TABLE VII

PARAMETERS OF DLS SIMULATION OF α-$LiIO_3$ (SPACE GROUP $P6_3$)

	Distances (Å)		Weight
Constraints	d(I–O)	1.803	2
	d(I---O)	2.908	0.5
	d(Li–O)[a]	2.117	1
	d(O–O)[b]	2.767	2
Refined variables	Cell dimensions (a,c)		
	z(Li), x(O), z(O)		

[a] For sake of simplicity, the two slightly different Li–O distances have been averaged.

[b] Oxygen–oxygen distances within the same (IO_3) group.

[3] Further information about distance least-squares simulations may be found in Refs. (*41–43*).

[4] All calculations performed with the program LATSUM (Pannetier, unpublished computer program, 1975) based on Bertaut's series ((*32*) and references quoted therein). Ionic charges Li (+1), I (+2.3), O (−1.1).

pected the minimum of energy corresponds to the maximum volume and to the experimental structure. Moreover, the slight asymmetry of the curve E_c vs θ indicates that an increase of temperature should decrease the average value of θ, in agreement with experiment. It is also worthwhile to mention that the maximum of volume (minimum of energy) for $\theta \neq 0$ is only due to the weak I---O bonds; indeed, a simulation without the constraint d(I---O) = 2.908 Å gives a maximum volume at $\theta = 0°$: the resulting structure is closely related to that of $CsNiCl_3$ (*45*) with Ni replacing Li and Cs shifted by ~c/4 from the iodine position.

A second result from this simple calculation (including the weak I---O bonds) is that the energy barrier corresponding to $\theta = 0°$ (i.e., to the transformation from one enantiomorph to the other by a cooperative rotation of all iodate groups) is very high. This was obviously not unexpected but, as the $\alpha \rightarrow \gamma$ transformation involves such a rotation of half of the pyramids, it strongly suggests that a fully cooperative motion of the iodate groups throughout the crystal is a rather unlikely mechanism for the phase transformation. However, the sluggishness of the transition which may spread over a range of about 50 K implies a gradual buildup of γ- from α-$LiIO_3$; the model presented in Section 5, although based only on geometrical arguments, may provide a plausible mechanism for the $\alpha \rightarrow \gamma$ phase transition.

Acknowledgments

We thank Dr. S. C. Abrahams for providing a copy of his manuscript (Ref. (*7*)) prior to publication. Thanks are also due to Dr. D. Bernard (Rennes) for performing the S.H.G. tests. One of us (J. P.) is indebted to Dr. Baerlocher (Zürich) and Dr. Dempsey (Newcastle) for providing a copy of the program DLS-76. The technical assistance of B. Michaux (Dijon) is gratefully acknowledged.

References

1. S. Matsumura, *Mater. Res. Bull.* **6,** 469 (1971).
2. H. Arend, M. Remoissenet, and W. Stäehlin, *Mater. Res. Bull.* **7,** 869 (1972).
3. M. Remoissenet, J. Garandet, and H. Arend, *Mater. Res. Bull.* **10,** 181 (1975).
4. M. Czank, H. Schulz, and H. G. Wiedmann, *Z. Kristallogr.* **143,** 99 (1976).
5. A. Rosenzweig and B. Morosin, *Acta Crystallogr.* **20,** 758 (1966).
6. J. L. De Boer, F. Van Bolhuis, R. Olthof-Hazekamp, and Aafje Vos, *Acta Crystallogr.* **21,** 841 (1966).
7. C. Svensson, J. Albertsson, R. Liminga, A. Kvick, and S. C. Abrahams, *J. Chem. Phys.* **78,** 7343 (1983).
8. E. Coquet, J.-M. Crettez, J. Pannetier, J. Bouillot, and J.-C. Damien, *Acta Crystallogr. Sect. B* **39,** 408 (1983).
9. J. M. Desvignes and M. Remoissenet, *Mater. Res. Bull.* **6,** 705 (1971).
10. H. Schulz, *Acta Crystallogr. Sect. B* **29,** 2285 (1973).
11. R. Liminga, C. Svensson, J. Albertsson, and S. C. Abrahams, *J. Chem. Phys.* **77**(7), 4222 (1982).
12. A. W. Hewat, Powder preparation program—ILL (1978).
13. Y. Y. Li, *Solid State Commun.* **45**(3), 251 (1983).
14. H. M. Rietveld, *J. Appl. Crystallogr.* **2,** 65 (1969).
15. A. W. Hewat, Harwell Report AERE-RF350 (1973).
16. L. Koester and H. Rauch, "Summary of Neutron Scattering Lengths," IAEA-Contract 2517/RB (1981).
17. P. J. Bendall, D. Phil. thesis, Oxford University (1980).
18. D. Bernard, private communication.
19. G. Cagliotti, A. Paoletti, and F. P. Ricci, *Nucl. Instrum.* **3,** 223 (1958).
20. I. D. Brown and R. D. Shannon, *Acta Crystallogr. Sect. A* **29,** 266 (1973).
21. A. Kirfel, G. Will, and R. F. Stewart, *Acta Crystallogr. Sect. B* **39,** 175 (1983).
22. F. Effenberger and J. Zemann, *Z. Kristallogr.* **150,** 133 (1970).
23. L. Pauling, *J. Amer. Chem. Soc.* **51,** 1010 (1929).
24. I. D. Brown, *in* "Structure and Bonding" (M. O'Keeffe and A. Navrotsky, Eds.), Vol. II, pp. 1–30, Academic Press, New York (1981).
25. W. H. Zachariasen, *J. Less-Common Met.* **62,** 1 (1978).
26. W. H. Zachariasen and R. A. Penneman, *J. Less-Common Met.* **69,** 369 (1980).
27. C. Svensson, S. C. Abrahams, and J. L. Bernstein, *J. Solid State Chem.* **36,** 195 (1981).
28. J. M. Crettez, J. P. Misset, and E. Coquet, *J. Chem. Phys.* **70,** 4194 (1979).
29. M. Peyrard, J. Garandet, and M. Remoissenet, *Solid State Commun.* **16,** 227 (1975).

30. A. Yu. Klimova, A. F. Konstantinova, Z. B. Perekalina, L. M. Belyaev, A. Yu. Kabaenkov, Z. P. Razmanova, and A. B. Vasiliev, *Sov. Phys. Crystallogr.* **27,** 680 (1982).
31. M. H. Cohen and F. Reif, *Solid State Phys.* **5,** 321 (1977).
32. E. F. Bertaut, *J. Phys. Chem. Solids* **39,** 97 (1978).
33. C. K. Coogan, *Aust. J. Chem.* **17,** 1 (1964); **20,** 2551 (1967).
34. H. C. Bolton, W. Fawcett, and I. D. C. Gurney, *Proc. Roy. Soc.* **80,** 199 (1962).
35. L. L. Makarov, A. B. Nikolsky, Ju. M. Zaitsev, Yu. F. Batrakov, Ju. I. Diatchenko, and A. K. Morozov, *J. Res. Inst. Catal. Hokkaido Univ. 24,* 102 (1976).
36. V. M. Sarnatskii, V. A. Shutilov, T. D. Levitskaya, B. I. Kidyarov, and P. L. Mitnitskii, *Sov. Phys. Solid State* **13,** 2021 (1972).
37. D. F. Baisa, S. V. Pogrebnyak, V. V. Safronov, and E. D. Chesnokov, *Sov. Phys. Crystallogr.* **22,** 180 (1977).
38. G. Denes, *J. Solid State Chem.* **37,** 16 (1981).
39. I. D. Brown, *J. Solid State Chem.* **11,** 214 (1974).
40. C. Baerlocher, A. Hepp, and W. M. Meier, "DLS-76: A Program for the Simulation of Crystal Structures by Geometric Refinement," Zürich (1977).
41. M. J. Dempsey and R. G. J. Strens, *in* "Physics and Chemistry of Minerals and Rocks" (R. G. J. Strens, Ed.), pp. 443–458, Wiley, New York (1976).
42. H. W. Baur, *Phys. Chem. Miner.* **2,** 3 (1977).
43. H. W. Baur, *in* "Structure and Bonding" (M. O'Keeffe and A. Navrotsky, Eds.), Vol. II, pp. 31–52, Academic Press, New York (1981).
44. M. O'Keeffe, *Acta Crystallogr. Sect. A* **33,** 924 (1977).
45. G. L. McPherson, T. J. Kistenmacher, and G. D. Stucky, *J. Chem. Phys.* **52,** 815 (1970).
46. D. M. Daraselia and A. Bräuer, *Phys. Status Solidi* 109b, 223 (1982).